

Occluded Video Instance Segmentation

Jiyang Qi^{1,2*}, Yan Gao^{2*}, Yao Hu², Xinggang Wang¹, Xiaoyu Liu², Xiang Bai¹,
Serge Belongie³, Alan Yuille⁴, Philip H.S. Torr⁵, Song Bai^{2,5†}

¹Huazhong University of Science and Technology, ²Alibaba Group, ³Cornell University,
⁴Johns Hopkins University, ⁵University of Oxford

Abstract

Can our video understanding systems perceive objects when a heavy occlusion exists in a scene?

To answer this question, we collect a large scale dataset called OVIS for occluded video instance segmentation, that is, to simultaneously detect, segment, and track instances in occluded scenes. OVIS consists of 296k high-quality instance masks from 25 semantic categories, where object occlusions usually occur. While our human vision systems can understand those occluded instances by contextual reasoning and association, our experiments suggest that current video understanding systems are not satisfying. On the OVIS dataset, the highest AP achieved by state-of-the-art algorithms is only 14.4, which reveals that we are still at a nascent stage for understanding objects, instances, and videos in a real-world scenario. Moreover, to complement missing object cues caused by occlusion, we propose a plug-and-play module called temporal feature calibration. Built upon MaskTrack R-CNN and SipMask, we report an AP of 15.2 and 15.0 respectively. The OVIS dataset is released at <http://songbai.site/ovis>, and the project code will be available soon.

1. Introduction

In the visual world, objects rarely occur in isolation. The psychophysical and computational studies have demonstrated [31, 15] that our vision systems perceive occluded objects by means of distinguishing actual boundaries of a given object (*a.k.a.*, intrinsic boundaries) from those caused by occlusion (*a.k.a.*, extrinsic boundaries), and then amodally explaining away the missing object cues. As shown in Fig. 1, we are able to complete the intrinsic contours coarsely with contextual reasoning, and sometimes, with prior knowledge.

The question then becomes, *can our video understanding*

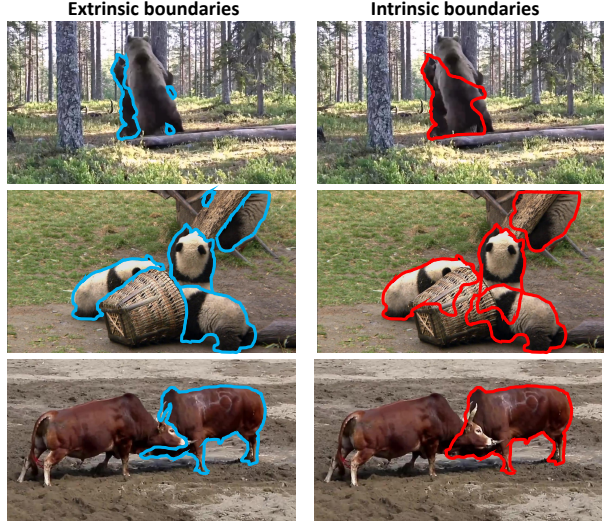


Figure 1. Illustrations of extrinsic (blue) and intrinsic (red) contours when object occlusions happen.

systems perceive occluded objects with comparable performance? Our work aims to explore this matter in the context of video instance segmentation, a popular task recently proposed in [49] that targets a comprehensive understanding of objects in videos. To this end, we explore a new and challenging scenario called **Occluded Video Instance Segmentation (OVIS)**, which requests a model to simultaneously detect, segment and track object instances in occluded scenes.

As the major contribution of this work, we collect a large scale dataset called OVIS, specifically for video instance segmentation in occluded scenes. While being the second video instance segmentation dataset after YouTube-VIS [49] with 131k masks, OVIS consists of 296k high-quality instance masks out of 25 commonly seen semantic categories. The most distinctive property of our OVIS dataset is that a large portion of objects is under various types of severe occlusions caused by different factors (see Fig. 2 for different types). Therefore, OVIS is a useful testbed to evaluate video instance segmentation models for dealing with heavy object occlusions.

*indicates equal contributions.

†Corresponding author. E-mail: songbai.site@gmail.com

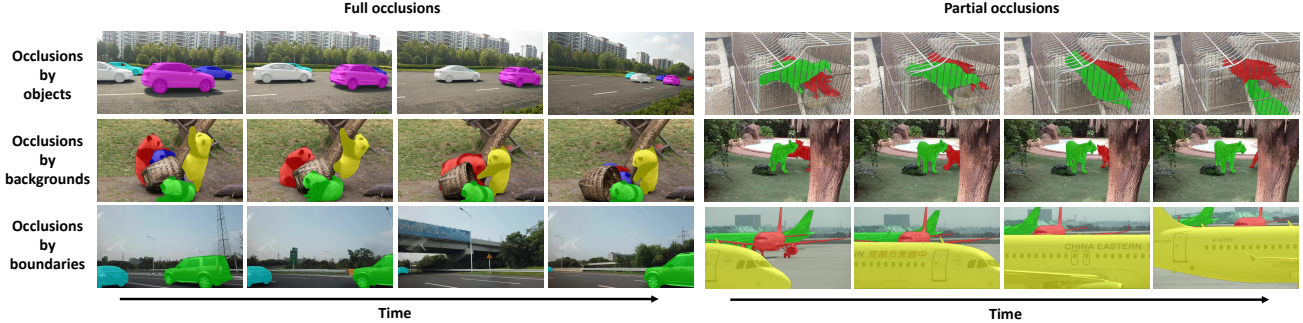


Figure 2. Various types of occlusions in OVIS. Full occlusion means the object totally disappears in some frames, while partial occlusion means that a part of the object is occluded. The causes of occlusions include objects, backgrounds, and frame boundaries.

To dissect the OVIS dataset, we conduct a thorough evaluation of 5 state-of-the-art algorithms whose code is publicly available, including FEELVOS [38], IoUTracker+ [49], MaskTrack R-CNN [49], SipMask [4], and STEM-Seg [1]. However, the experimental results suggest that current video understanding systems fall behind the capability of human beings in terms of occlusion perception. The highest AP is only 14.4 achieved by [1]. In this sense, we are still far from deploying those techniques into practical applications, especially considering the complexity and diversity of scenes in the real visual world.

To address the occlusion issue, we also propose a simple baseline module called temporal feature calibration. For a given query frame in a video, we resort to a reference frame to complement its missing object cues. Specifically, the proposed module learns a calibration offset for the reference frame with the guidance of the query frame, and then the offset is used to adjust the feature embedding of the reference frame via deformable convolution [8]. The refined reference embedding is used in turn to assist the object recognition of the query frame. Our module is a highly flexible plug-in. While applied to MaskTrack R-CNN [49] and SipMask [4] respectively, we report an AP of 15.2 and 15.0, significantly outperforming the corresponding baselines by 2.6 and 2.9 in AP respectively.

To summarize, our contributions are three-fold:

- We advance video instance segmentation by releasing a new benchmark dataset named **OVIS** (short for **Occluded Video Instance Segmentation**). OVIS is designed with the philosophy of perceiving object occlusions in videos, which could reveal the complexity and the diversity of real-world scenes.
- We streamline the research over the OVIS dataset by conducting a comprehensive evaluation of 5 state-of-the-art video instance segmentation algorithms, which could be a baseline reference for future research in OVIS.
- We propose a plug-and-play module to alleviate the

occlusion issue. While applied to MaskTrack R-CNN [49], we report an AP of 15.2 on OVIS and 32.1 on YouTube-VIS respectively, outperforming a series of state-of-the-art methods. When applied to SipMask [4], we report a AP of 15.0 on OVIS and 35.0 on YouTube-VIS.

2. Related Work

Our work focuses on **Video Instance Segmentation** in occluded scenes. The most relevant work to ours is [49], which formally defines the concept of video instance segmentation and releases the first dataset called YouTube-VIS. Built upon the large-scale video object segmentation dataset YouTube-VOS [47], the YouTube-VIS dataset contains a total of 2,883 videos, 4,883 instances, and 131k masks in 40 categories. Compared with the YouTube-VIS dataset, OVIS aims to construct a more challenging video instance segmentation dataset with severe occlusions.

Since the release of the YouTube-VIS dataset, video instance segmentation has attracted great attention in the computer vision community, arising a series of algorithms recently [49, 4, 1, 2, 27, 30, 41, 11]. MaskTrack R-CNN [49] is the first unified model for video instance segmentation. It achieves video instance segmentation by adding a tracking branch to the popular image instance segmentation method Mask R-CNN [13]. Lin *et al.* [27] propose a modified variational auto-encoder architecture built on the top of Mask R-CNN. MaskProp [2] is also a video extension of Mask R-CNN which adds a mask propagation branch to propagate masks to adjacent frames, and then tracks instances by the propagated masks. SipMask [4] extends single-stage image instance segmentation to the video level by adding a fully-convolutional branch for tracking instances. Different from those top-down methods, STEM-Seg [1] proposes a bottom-up method, which performs video instance segmentation by clustering the pixels of the same instance. Our method adopts MaskTrack R-CNN [49] and SipMask [4] as the baselines, and endows them with the ability to alleviate object occlusions. By adding the proposed feature calibra-

tion module, the performance is significantly improved in occluded scenes.

Meanwhile, our work is also relevant to several other tasks, including:

Video Object Segmentation. Video object segmentation (VOS) is a popular task in video analysis. According to whether to provide the mask for the first frame, VOS can be divided into semi-supervised and unsupervised scenarios. Semi-supervised VOS [40, 19, 25, 34, 16, 18, 35, 26] aims to track and segment a given object with a mask. Many Semi-supervised VOS methods [40, 19, 25] adopt an online learning manner which fine-tunes the network on the mask of the first frame during inference. Recently, some other works [34, 16, 18, 35, 26] aim to avoid online learning for the sake of faster inference speed. Unsupervised VOS methods [24, 42, 37] aim to segment the primary objects in a video without the first frame annotations. Different from video instance segmentation that needs to classify objects, both unsupervised and semi-supervised VOS does not distinguish semantic categories.

Video Semantic Segmentation. Video semantic segmentation requires semantic segmentation for each frame in a video. LSTM [10], GRU [33], and optical flow [52] are introduced to leverage temporal contextual information for more accurate or faster video semantic segmentation. Video semantic segmentation does not require distinguishing instances and tracking objects across frames.

Video Panoptic Segmentation. Dahun *et al.* [20] define a video extension of panoptic segmentation [21], which requires generating consistent panoptic segmentation, and in the meantime, associating instances across frames.

Multi-Object Tracking and Segmentation. Multi-object tracking and segmentation (MOTS) [39] task extends Multi-Object Tracking (MOT) [36] from a bounding box level to a pixel level. Paul *et al.* [39] release the KITTI MOTS and MOTSChallenge dataset, and propose Track R-CNN that extends Mask R-CNN by 3D convolutions to incorporate temporal context and an extra tracking branch for object tracking. Xu *et al.* [48] release the ApolloScape dataset which provides more crowded scenes and proposes a new track-by-points paradigm.

Our work is of course relevant to some image-level recognition tasks, such as semantic segmentation [29, 6, 7], instance segmentation [13, 17, 22], panoptic segmentation [21, 46, 23], large vocabulary instance segmentation [12, 44], *etc.*

3. OVIS Dataset

Given an input video, video instance segmentation requires detecting, segmenting, and tracking object instances simultaneously from a predefined set of object categories.

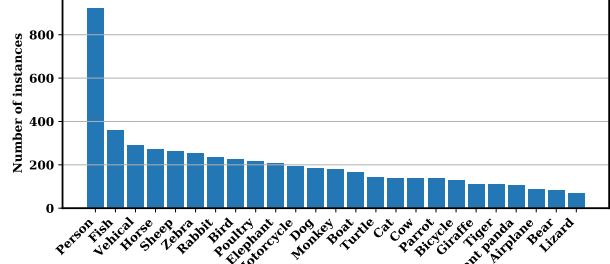


Figure 3. Number of instances per category in the OVIS dataset.

An algorithm is supposed to output the class label, confidence score, and a sequence of binary masks of each instance.

The focus of this work is on collecting a large scale benchmark dataset for video instance segmentation with severe object occlusions. In this section, we mainly review the data collection process, the annotation process, and the dataset statistics.

3.1. Video Collection

We begin with 25 semantic categories, including *Person*, *Bird*, *Cat*, *Dog*, *Horse*, *Sheep*, *Cow*, *Elephant*, *Bear*, *Zebra*, *Giraffe*, *Poultry*, *Giant panda*, *Lizard*, *Parrot*, *Monkey*, *Rabbit*, *Tiger*, *Fish*, *Turtle*, *Bicycle*, *Motorcycle*, *Airplane*, *Boat*, and *Vehicle*. The categories are carefully chosen mainly for three motivations: 1) most of them are animals, because movement will lead to severe occlusions, 2) they are commonly seen in our life, 3) these categories have a high overlap with popular large-scale image instance segmentation datasets [28, 12] so that models trained on those datasets are easier to be transferred. The number of instances per category is given in Fig. 3.

As the dataset is to study the capability of our video understanding systems to perceive occlusions, we ask the annotation team to 1) exclude those videos, where only one single object stands in the foreground; 2) exclude those videos with a clean background; 3) exclude those videos, where the complete contour of objects is visible all the time. In the meantime, ensure that each video shall have at least one occlusion type out of *occlusion by object*, *occlusion by backgrounds*, and *occlusion by boundaries* (see Fig. 2 for illustrations). Some other objective rules include: 1) video length is generally between 5s and 60s, and 2) video resolution is generally 1920×1080 ;

After applying the objective rules, the annotation team delivers 8,644 video candidates and our research team only accepts 901 videos after a careful re-check. It should be mentioned that due to the stringent standard of video collection, the pass rate is as low as 10%.

Dataset	YouTube-VIS	OVIS (ours)
Masks	131k	296k
Categories	40	25
Videos	2,883	901
Instances	4,883	5,223
Video duration (s)	4.63	12.77
Instance duration (s)	4.47	10.05
mBOR*	0.07	0.22
Objects per frame	1.64	4.72
Instances per video	1.69	5.80

Table 1. Comparing OVIS with YouTube-VIS in terms of statistics. See Eq. (1) for the definition of mBOR. * means the value of YouTube-VIS is estimated from the training set.

3.2. Annotation

Given an accepted video, the annotation team is asked to exhaustively annotate all the objects belonging to the pre-defined category set. Each object is given an instance identity and a class label. In addition to some common rules (*e.g.*, no ID switch, mask fitness ≤ 1 pixel), the annotation team is trained with several criteria particularly about occlusions: 1) if an existing object disappears because of full occlusions, then re-appears, the instance identity should keep the same; 2) if a new instance appears in an in-between frame, a new instance identity is needed; and 3) the case of “object re-appears” and “new instances” should be distinguishable by you after you watch the contextual frames therein. All the videos are annotated per 5 frames, which results in that the granularity ranges from 3 to 6 fps.

Each video is handled by one annotator to get the initial annotation, and the initial annotation is then passed to another annotator to check and correct if necessary. The final annotations will be examined by our research team and sent back for revision if deemed below the required quality.

While being designed for video instance segmentation, it should be noted that OVIS is also suitable for evaluating video object segmentation in either a semi-supervised or unsupervised fashion, and object tracking since the bounding-box annotation is also provided. The relevant experimental settings will be explored as part of our future work.

3.3. Dataset Statistics

As YouTube-VIS [49] is the only dataset that is specifically designed for video instance segmentation nowadays, we analyze the data statistics of our OVIS dataset with YouTube-VIS as a reference in Table 1. Note that some statistics, marked with *, of YouTube-VIS is only calculated from the training set because only the annotation of the training set is publicly available. Nevertheless, considering the training set occupies 78% of the whole dataset, those statistics could still reflect the properties of YouTube-VIS roughly.

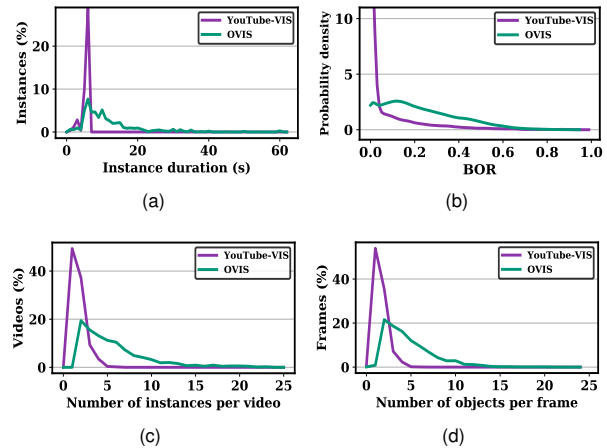


Figure 4. Comparison of OVIS with YouTube-VIS, including the distribution of instance duration (a), BOR (b), the number of instances per video (c), and the number of objects per frame (d)

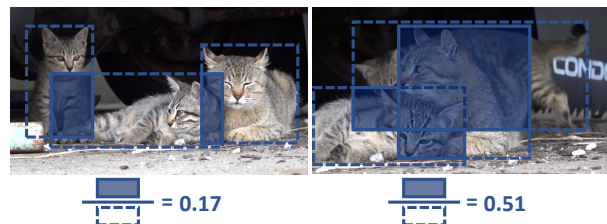


Figure 5. Visualization of occlusions with different BOR values.

In terms of basic and high-level statistics, OVIS contains 296k masks and 5,223 instances, which is larger than YouTube-VIS that has 131k masks and 4,883 instances. Nonetheless, OVIS has fewer videos than YouTube-VIS as our design philosophy favors long videos and instances so as to preserve enough motion and occlusion scenarios.

As is shown, the average video duration and the average instance duration of OVIS are 12.77s and 10.05s respectively. Fig. 4(a) presents the distribution of instance duration, which shows that all instances in YouTube-VIS last less than 6s. Long videos and instances increase the difficulty of tracking and the ability of long-term tracking is required.

As for object occlusions, it is somewhat problematic to quantitatively measure the degree. To remedy this, we define a metric named Bounding-box Occlusion Rate (BOR). Given a video frame with N objects denoted by bounding boxes $\{\mathbf{B}_1, \mathbf{B}_2, \dots, \mathbf{B}_N\}$, we compute the BOR for this frame as

$$\text{BOR} = \frac{|\bigcup_{1 \leq i < j \leq N} \mathbf{B}_i \cap \mathbf{B}_j|}{|\bigcup_{1 \leq i \leq N} \mathbf{B}_i|}, \quad (1)$$

where the numerator means the area sum of the intersection between any two or more bounding boxes. In other words, we exclude those positions which only appear in an individual bounding box. The denominator means the area

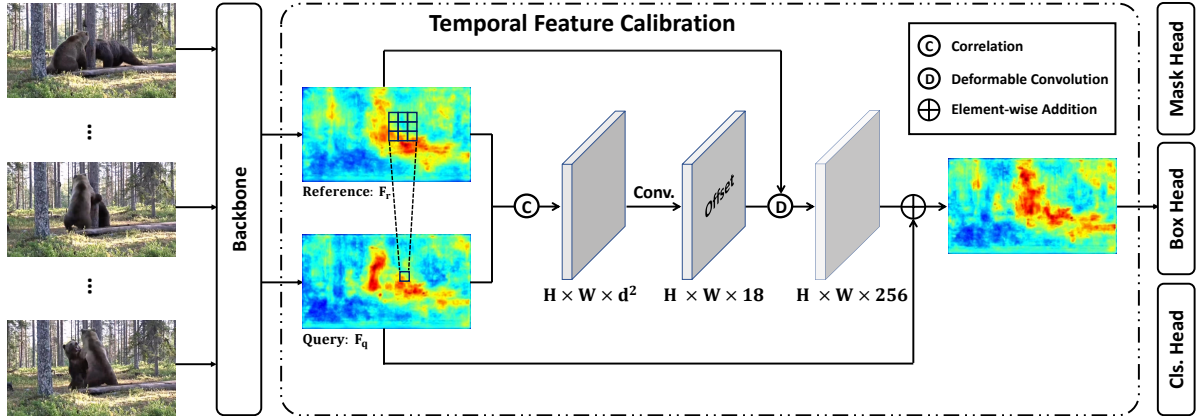


Figure 6. The pipeline of temporal feature calibration, which can be inserted into different video instance segmentation models by changing the prediction head. We verify this flexibility using MaskTrack R-CNN and SipMask in our experiments.

of the union of all the bounding boxes. An illustration is given in Fig. 5, which shows the larger the BOR value is, the heavier the occlusion is.

Then we utilize mBOR, the average value of BORs of all the frames in a dataset (frames that do not contain any objects are ignored), to characterize the dataset in terms of the occlusion. As shown in Table 1, the mBOR of OVIS is 0.22, much higher than that of YouTube-VIS 0.07. The BOR distribution is further compared in Fig. 4(b). As can be seen, most frames in YouTube-VIS are located in the region where $BOR \leq 0.1$ and a small number of frames' BOR are greater than 0.1. In comparison, the BOR of about half frames in OVIS is no less than 0.2. It supports the focus of our work, that is, to explore the ability of video instance segmentation models in handling occlusion scenes. However, it should be mentioned here that BOR cannot involve all the occlusion types shown in Fig. 2, but is mainly targeted at occlusion by objects. Therefore, *mBOR could serve as an effective indicator for occlusion degrees, but only reflect the occlusion degree in a partial or rough way*.

In addition to long videos&instances and severe occlusions, OVIS features crowded scenes, which is a natural effect of heavy occlusions. OVIS has 5.80 instances per video and 4.72 objects per frame, while those two values are 1.69 and 1.64 respectively in YouTube-VIS. The comparison of the two distributions is further depicted in Fig. 4(c) and Fig. 4(d).

4. Proposed Approach

We build our method based on MaskTrack R-CNN [49], considering it is the official baseline approach released along with the YouTube-VIS dataset while being a representative of algorithms in this field. In this section, we first revisit MaskTrack R-CNN briefly, then elaborate the details of our method. Note that our method is also compatible with other video instance segmentation models (*e.g.*, Sip-

Mask [4]) and refer to the experiments for details.

4.1. MaskTrack R-CNN Revisited

Based on Mask R-CNN [13], MaskTrack R-CNN fulfills video instance segmentation by leveraging four branches. Basically, the three branches for object classification, bounding box regression, and mask generation keep the same as Mask R-CNN, which are applied to every single frame. The fourth tracking branch is responsible for tracking objects across frames. Suppose there are N instances identified from previous frames, the candidate box i in the current frame will be assigned to the label n , with the assignment probability defined as

$$p_i(n) = \begin{cases} \frac{e^{f_i^T f_n}}{1 + \sum_{j=1}^N e^{f_i^T f_j}} & n \in [1, N] \\ \frac{1}{1 + \sum_{j=1}^N e^{f_i^T f_j}} & n = 0 \end{cases} \quad (2)$$

where $1 \leq n \leq N$ indicates the candidate is associated to one of the N instances and $n = 0$ means the candidate is treated as a new identity. f_i and f_j ($j \in [1, N]$) denote the feature embedding of the candidate and the N pre-identified instances, respectively. The cross-entropy loss is used here in a way of multi-class classification.

The overall training loss function used is a combination of the Mask R-CNN losses and the tracking loss. During inference, MaskTrack R-CNN maintains a memory to store the feature vectors of existing instances. For more details (*e.g.*, memory update, inference strategy, model setup), please refer to [49].

4.2. Temporal Feature Calibration

One of the keys to tackling occlusion is to complement the missing object cues. In a video that has a temporal dimension, a mild assumption is that usually, the missing object cues in the current frame may have appeared in adjacent frames. Hence, it is natural to leverage adjacent frames

Methods	OVIS validation set					OVIS test set				
	AP	AP ₅₀	AP ₇₅	AR ₁	AR ₁₀	AP	AP ₅₀	AP ₇₅	AR ₁	AR ₁₀
FEELVOS [38]	9.6	22.3	7.6	7.4	14.8	11.5	23.7	8.4	9.2	16.3
IoUTracker+ [49]	7.3	17.9	5.5	6.1	15.1	9.5	18.8	10.0	6.6	16.5
MaskTrack R-CNN [49]	10.9	26.0	8.1	8.3	15.2	12.6	27.3	10.7	8.3	16.6
SipMask [4]	10.3	25.4	7.8	7.9	15.8	12.1	24.9	11.1	8.3	17.0
STEM-Seg [1]	13.8	32.1	11.9	9.1	20.0	14.4	30.0	13.0	10.1	20.6
CSipMask (ours)	13.9	30.7	11.9	9.4	19.4	15.0	30.4	13.4	9.7	20.8
CMaskTrack R-CNN (ours)	14.9	32.4	12.5	9.1	19.5	15.2	31.2	14.3	10.1	20.1

Table 2. Quantitative comparison with state-of-the-art methods on the OVIS validation and test set.

Methods	YouTube-VIS validation set				
	AP	AP ₅₀	AP ₇₅	AR ₁	AR ₁₀
FEELVOS [38]	26.9	42.0	29.7	29.9	33.4
IoUTracker+ [49]	23.6	39.2	25.5	26.2	30.9
OSMN [50]	27.5	45.1	29.1	28.6	33.1
DeepSORT [43]	26.1	42.9	26.1	27.8	31.3
MaskTrack R-CNN [49]	30.3	51.1	32.6	31.0	35.5
SipMask [4]	32.5	53.0	33.3	33.5	38.9
STEM-Seg [1]	30.6	50.7	33.5	31.6	37.1
CMaskTrack R-CNN	32.1	52.3	34.4	32.8	37.6
CSipMask	35.0	55.0	38.1	35.8	41.4

Table 3. Quantitative comparison with state-of-the-art methods on the YouTube-VIS validation set.

to alleviate occlusions. However, caused by motions, the features of different frames are not aligned in the spatial dimension. Things get much worse because of the existence of severe occlusions. To solve this issue, we propose an easy plug-in called temporal feature calibration as illustrated in Fig. 6.

Denote by $\mathbf{F}_q \in \mathbb{R}^{H \times W \times C}$ and $\mathbf{F}_r \in \mathbb{R}^{H \times W \times C}$ the feature tensor of the query frame (called target or current frame in some literature) and a reference frame, respectively. The feature calibration first computes the spatial correlation [9] between \mathbf{F}_q and \mathbf{F}_r . Given a location \mathbf{x}_q in \mathbf{F}_q and \mathbf{x}_r in \mathbf{F}_r , we compute

$$\mathbf{c}(\mathbf{x}_q, \mathbf{x}_r) = \sum_{o \in [-k, k] \times [-k, k]} \mathbf{F}_q(\mathbf{x}_q + o) \mathbf{F}_r(\mathbf{x}_r + o)^T, \quad (3)$$

The above operation will transverse the $d \times d$ area centered on \mathbf{x}_q , then outputs a d^2 -dimensional vector.

After enumerating all the positions in \mathbf{F}_q , we obtain $\mathbf{C} \in \mathbb{R}^{H \times W \times d^2}$ and forward it into multiple stacked convolution layers to get the spatial calibration offset $\mathbf{D} \in \mathbb{R}^{H \times W \times 18}$. We then obtain a calibrated version of \mathbf{F}_r by applying deformable convolutions with \mathbf{D} as the spatial calibration offset, which is denoted as $\bar{\mathbf{F}}_r$. At last, we fuse the calibrated reference feature $\bar{\mathbf{F}}_r$ with the query feature \mathbf{F}_q by element-wise addition for the localization, classification and segmentation of the current frame afterward.

During training, for each query frame \mathbf{F}_q , we randomly

sample a reference frame \mathbf{F}_r from the same video. In order to ensure that the reference frame has a strong spatial correspondence with the query frame, the sampling is only done locally within $\epsilon_{\text{train}} = 5$ frames. Since the temporal feature calibration is differentiable, it can be trained end-to-end by the original detection and segmentation loss. When inference, all frames adjacent to the query frame within the range $\epsilon_{\text{test}} = 3$ are taken as reference frames. We linearly fuse the classification confidences, regression bounding box coordinates, and segmentation masks obtained from each reference frame and output the final results for the query frame.

In the experiments, we denote our method as **CMask-Track R-CNN** and **CSipMask**, when Calibrating **Mask-Track R-CNN** [49] models and Calibrating **SipMask** [4] models, respectively.

5. Experiments

The experiments are mainly focused on two aspects, including 1) a comprehensive evaluation of 5 existing video instance segmentation algorithms to benchmark the baseline performance of our OVIS dataset, and 2) a performance comparison between our method (CMaskTrack R-CNN and CSipMask) and state-of-the-art algorithms in both OVIS and YouTube-VIS.

5.1. Dataset, Metric and Implementation Details

The YouTube-VIS dataset [49] has 2,238 training videos, 302 validation videos, and 343 test videos. We train our model on the training set and report the performance on the validation set. On the newly collected OVIS dataset, the whole dataset is randomly divided into 607 training videos, 140 validation videos, and 154 testing videos. Following previous methods [49], we use average precision (AP) at different intersection-over-union (IoU) thresholds and average recall (AR) as the evaluation metrics. The mean value of APs is also employed.

We adopt ResNet-50-FPN [14] as backbone for all our experiments. The model is initialized by Mask R-CNN which is pre-trained on MS-COCO [28]. Three convolution layers of kernel size 3×3 are used in the module for



Figure 7. Qualitative evaluation of CMaskTrack R-CNN on OVIS. Each row presents the results of 5 frames in a video sequence. (a)-(d) are 4 successful cases and (e)-(f) are failure cases.

temporal feature calibration. The training epoch is set to 12, and the initial learning rate is set to 0.005 and decays with a factor of 10 at epoch 8 and 11. All frames are resized to 640×360 during both training and inference.

5.2. Comparison with State-of-the-art

On the OVIS dataset, we first produce the performance of several state-of-the-art algorithms whose code is publicly available¹, including mask propagation methods (*e.g.*, FELVOS [38]), track-by-detect methods (*e.g.*, IoUTracker+ [49]), and recently proposed end-to-end methods (*e.g.*, MaskTrack R-CNN [49], SipMask [4], and STEm-Seg [1]).

As presented in Table 2 and Table 3, all those methods encounter a performance degradation of at least 50% on OVIS compared with that on YouTube-VIS. For example, the AP of SipMask [4] decreases from 32.5 to 12.1 and that of STEm-Seg [1] decreases from 30.6 to 14.4. It firmly suggests that further attention should be paid to video instance segmentation in the real world where occlusions extensively happen.

Benefiting from 3D convolutional layers and the bottom-up architecture, STEm-Seg surpasses other methods on OVIS and reports an AP of 14.4. Our interpretation is that

3D convolution is conducive to sensing temporal context, and the bottom-up architecture avoids the detection process which is difficult in occluded scenes.

By leveraging the feature calibration module, the performance on OVIS is significantly improved. Our CMaskTrack R-CNN leads to an AP improvement of 2.6 over MaskTrack R-CNN (12.6 vs. 15.2), and our CSipMask leads to an AP improvement of 2.9 over SipMask (12.1 vs. 15.0). Both achievements are superior to that of STEm-Seg, by a margin of 0.8 and 0.6 in terms of AP, respectively.

Some evaluation examples of CMaskTrack R-CNN on OVIS are given in Fig. 7, including 4 successful cases (a)-(d) and 2 failure cases (e)-(f). In (a), our model successfully tracks the bear in the yellow mask, which is partially occluded by another object, *i.e.*, the bear in the purple mask, and the background, *i.e.*, the tree. In (c), we present a crowded scene where almost all the ducks are correctly detected and tracked, with only a missing detection on the left-most duck in the 2nd frame. However, it is surprising to see that the duck is re-tracked in later frames, which reveal that the temporal cues are well captured by our model. In (d), the car in the yellow mask first blocks the car in the red mask entirely in the 2nd frame, then is entirely blocked by the car in the purple mask in the 4th frame. Even in this extreme case, all the cars are well tracked. In (e), two persons and two bicycles heavily overlap with each other. Our

¹The performance of some methods is also being produced by the authors of the corresponding papers, which will be updated afterward.

model fails to track the person and segment the bicycle. In (f), although humans could sense that there are two persons with hat in the bottom, our model cannot detect and track them because the appeared visual cues are inadequate.

We further evaluate the proposed CMaskTrack R-CNN and CSipMask on the YouTube-VIS dataset. As shown in Table 3, CMaskTrack R-CNN and CSipMask surpass the corresponding baseline by 1.8 and 2.5 in terms of AP, respectively, which demonstrates the flexibility and the generalization power of the proposed feature calibration module. Moreover, our methods also beat other representative methods by a larger margin, including Deep-SORT [43], STEm-Seg [1], etc. In [2], Gedas *et al.* propose MaskProp by replacing the bounding-box level tracking in MaskTrack R-CNN by a novel mask propagation mechanism. By using a larger backbone (STSN [3]-ResNeXt-101-64x4d [45]), a better detection network (HybridTask Cascade Network [5]), higher resolution inputs for segmentation network, and more training iterations, it reports a much higher AP of 46.6 on YouTube-VIS. We believe that our module is also pluggable to this strong baseline and better performance could be achieved. Meanwhile, it is also interesting to evaluate the performance of MaskProp on OVIS after its code is released.

5.3. Discussions

Ablation Study. We study the temporal feature calibration module with a few alternatives. The first option is a naive combination, which sums up the feature of the query frame and the reference frame without any feature alignment. The second option is to replace the correlation operation in our module by calculating the element-wise difference between feature maps, which is similar to the operation used in [2]. We denote the two options as “Add” and “Difference”, respectively and our module as “Calibration” in Fig. 8.

As we can see, with both models, “Add” achieves the poorest performance, which shows that a kind of feature calibration between different frames is necessary and beneficial to an accurate prediction of video instance segmentation. Meanwhile, “Calibration” consistently outperforms “Difference” with a decent performance boost. For example, “Calibration” achieves an AP of 15.2, an improvement of 0.8 over “Difference” with MaskTrack R-CNN as the base model, and achieves an AP of 13.9, an improvement of 0.9 over “Difference” with SipMask as the base model. We argue that the correlation operation is able to provide a richer context for feature calibration because it calculates the similarity between the query position and its neighboring positions, while the element-wise difference only considers the difference between the same positions.

Oracle Results. In addition, we conduct an experiment to explore the upper bounds of our method on OVIS by replacing the image level predictions with ground-truth. Specifi-

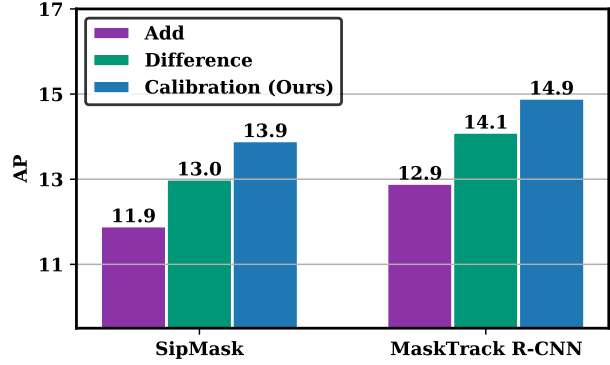


Figure 8. Ablation study of temporal feature calibration on the OVIS validation set. “Add” means adding feature maps directly without calibration. “Difference” means generating the calibration offset based on the element-wise difference between feature maps.

cally, we use ground-truth bounding boxes, masks and categories to replace the predictions by CMaskTrack R-CNN, track those ground-truth bounding boxes with the tracking branch, then obtain final instances. By doing so, we achieve an AP of 58.4 and an AR₁₀ of 66.1, which demonstrates that the image level prediction is critical for the performance of occluded video instance segmentation.

6. Conclusions

In this work, we target video instance segmentation in occluded scenes, and accordingly contribute a large-scale dataset called OVIS. OVIS consists of 296k high-quality instance masks of 5,223 heavily occluded instances. While being the second benchmark dataset after YouTube-VIS, OVIS is designed to examine the ability of current video understanding systems in terms of handling object occlusions. A general conclusion comes to that the baseline performance on OVIS is far below that on YouTube-VIS, which suggests that more effort should be devoted in the future to tackling object occlusions or de-occluding objects [51]. We also explore ways about leveraging temporal context cues to alleviate the occlusion matter, and report an AP of 15.2 on OVIS and 35.0 on YouTube-VIS, a remarkable gain over the state-of-the-art algorithms.

In the future, we are interested in formalizing the experimental track of OVIS for video object segmentation, either in an unsupervised, semi-supervised, or interactive setting. It is also of paramount importance to extend OVIS to video panoptic segmentation [20]. As we can see from Fig. 2, a type of occlusion is caused by the background, therefore in this case, heavy occlusions will also affect the prediction of background stuff. At last, synthetic occluded data [32] requires further exploration. We believe the OVIS dataset will trigger more research in understanding videos in complex and diverse scenes.

References

[1] Ali Athar, Sabarinath Mahadevan, Aljoša Ošep, Laura Leal-Taixé, and Bastian Leibe. Stem-seg: Spatio-temporal embeddings for instance segmentation in videos. In *ECCV*, 2020. 2, 6, 7, 8

[2] Gedas Bertasius and Lorenzo Torresani. Classifying, segmenting, and tracking object instances in video with mask propagation. In *CVPR*, 2020. 2, 8

[3] Gedas Bertasius, Lorenzo Torresani, and Jianbo Shi. Object detection in video with spatiotemporal sampling networks. In *ECCV*, 2018. 8

[4] Jiale Cao, Rao Muhammad Anwer, Hisham Cholakkal, Fahad Shahbaz Khan, Yanwei Pang, and Ling Shao. Sipmask: Spatial information preservation for fast image and video instance segmentation. In *ECCV*, 2020. 2, 5, 6, 7

[5] Kai Chen, Jiangmiao Pang, Jiaqi Wang, Yu Xiong, Xiaoxiao Li, Shuyang Sun, Wansen Feng, Ziwei Liu, Jianping Shi, Wanli Ouyang, et al. Hybrid task cascade for instance segmentation. In *CVPR*, pages 4974–4983, 2019. 8

[6] Liang-Chieh Chen, George Papandreou, Iasonas Kokkinos, Kevin Murphy, and Alan L Yuille. Deeplab: Semantic image segmentation with deep convolutional nets, atrous convolution, and fully connected crfs. *IEEE TPAMI*, 40(4):834–848, 2017. 3

[7] Liang-Chieh Chen, Yukun Zhu, George Papandreou, Florian Schroff, and Hartwig Adam. Encoder-decoder with atrous separable convolution for semantic image segmentation. In *ECCV*, 2018. 3

[8] Jifeng Dai, Haozhi Qi, Yuwen Xiong, Yi Li, Guodong Zhang, Han Hu, and Yichen Wei. Deformable convolutional networks. In *ICCV*, 2017. 2

[9] Alexey Dosovitskiy, Philipp Fischer, Eddy Ilg, Philip Hausser, Caner Hazirbas, Vladimir Golkov, Patrick Van Der Smagt, Daniel Cremers, and Thomas Brox. Flownet: Learning optical flow with convolutional networks. In *CVPR*, 2015. 6

[10] Mohsen Fayyaz, Mohammad Hajizadeh Saffar, Mohammad Sabokrou, Mahmood Fathy, Reinhard Klette, and Fay Huang. Stfcn: spatio-temporal fcn for semantic video segmentation. In *ACCV*, 2016. 3

[11] Qianyu Feng, Zongxin Yang, Peike Li, Yunchao Wei, and Yi Yang. Dual embedding learning for video instance segmentation. In *ICCVW*, 2019. 2

[12] Agrim Gupta, Piotr Dollar, and Ross Girshick. Lvis: A dataset for large vocabulary instance segmentation. In *CVPR*, 2019. 3

[13] Kaiming He, Georgia Gkioxari, Piotr Dollár, and Ross Girshick. Mask r-cnn. In *CVPR*, 2017. 2, 3, 5

[14] Kaiming He, Xiangyu Zhang, Shaoqing Ren, and Jian Sun. Deep residual learning for image recognition. In *CVPR*, 2016. 6

[15] Jay Hegdé, Fang Fang, Scott O Murray, and Daniel Kersten. Preferential responses to occluded objects in the human visual cortex. *JOV*, 8(4):16–16, 2008. 1

[16] Yuan Ting Hu, Jia Bin Huang, and Alexander G. Schwing. Videomatch: Matching based video object segmentation. In *ECCV*, 2018. 3

[17] Zhaojin Huang, Lichao Huang, Yongchao Gong, Chang Huang, and Xinggang Wang. Mask scoring r-cnn. In *CVPR*, 2019. 3

[18] Joakim Johnander, Martin Danelljan, Emil Brissman, Fahad Shahbaz Khan, and Michael Felsberg. A generative appearance model for end-to-end video object segmentation. In *CVPR*, 2019. 3

[19] Anna Khoreva, Federico Perazzi, Rodrigo Benenson, Bernt Schiele, and Alexander Sorkine-Hornung. Learning video object segmentation from static images. In *CVPR*, 2017. 3

[20] Dahun Kim, Sanghyun Woo, Joon-Young Lee, and In So Kweon. Video panoptic segmentation. In *CVPR*, 2020. 3, 8

[21] Alexander Kirillov, Kaiming He, Ross Girshick, Carsten Rother, and Piotr Dollár. Panoptic segmentation. In *CVPR*, 2019. 3

[22] Alexander Kirillov, Yuxin Wu, Kaiming He, and Ross Girshick. Pointrend: Image segmentation as rendering. In *CVPR*, 2020. 3

[23] Qizhu Li, Xiaojuan Qi, and Philip HS Torr. Unifying training and inference for panoptic segmentation. In *CVPR*, 2020. 3

[24] Siyang Li, Bryan Seybold, Alexey Vorobyov, Alireza Fathi, and C. C. Jay Kuo. Instance embedding transfer to unsupervised video object segmentation. In *CVPR*, 2018. 3

[25] Xiaoxiao Li and Chen Change Loy. Video object segmentation with joint re-identification and attention-aware mask propagation. In *ECCV*, 2018. 3

[26] Yuxi Li, Ning Xu, Jinlong Peng, John See, and Weiyao Lin. Delving into the cyclic mechanism in semi-supervised video object segmentation. *NeurIPS*, 33, 2020. 3

[27] Chung-Ching Lin, Ying Hung, Rogerio Feris, and Linglin He. Video instance segmentation tracking with a modified vae architecture. In *CVPR*, 2020. 2

[28] Tsung-Yi Lin, Michael Maire, Serge J Belongie, James Hays, Pietro Perona, Deva Ramanan, Piotr Dollár, and C Lawrence Zitnick. Microsoft coco: Common objects in context. In *ECCV*, 2014. 3, 6

[29] Jonathan Long, Evan Shelhamer, and Trevor Darrell. Fully convolutional networks for semantic segmentation. In *CVPR*, 2015. 3

[30] Jonathon Luiten, Philip Torr, and Bastian Leibe. Video instance segmentation 2019: A winning approach for combined detection, segmentation, classification and tracking. In *ICCVW*, 2019. 2

[31] Ken Nakayama, Shinsuke Shimojo, and Gerald H Silverman. Stereoscopic depth: its relation to image segmentation, grouping, and the recognition of occluded objects. *Perception*, 18(1):55–68, 1989. 1

[32] Sergey I Nikolenko. Synthetic data for deep learning. *arXiv*, 2019. 8

[33] David Nilsson and Cristian Sminchisescu. Semantic video segmentation by gated recurrent flow propagation. In *CVPR*, 2018. 3

[34] Seoung Wug Oh, Joon Young Lee, Kalyan Sunkavalli, and Seon Joo Kim. Fast video object segmentation by reference-guided mask propagation. In *CVPR*, 2018. 3

[35] Seoung Wug Oh, Joon Young Lee, Ning Xu, and Seon Joo Kim. Video object segmentation using space-time memory networks. In *ICCV*, 2019. 3

[36] Arnold WM Smeulders, Dung M Chu, Rita Cucchiara, Simone Calderara, Afshin Dehghan, and Mubarak Shah. Visual tracking: An experimental survey. *IEEE TPAMI*, 36(7):1442–1468, 2013. 3

[37] Pavel Tokmakov, Karteek Alahari, and Cordelia Schmid. Learning motion patterns in videos. In *CVPR*, 2017. 3

[38] Paul Voigtlaender, Yuning Chai, Florian Schroff, Hartwig Adam, Bastian Leibe, and Liang-Chieh Chen. Feelvos: Fast end-to-end embedding learning for video object segmentation. In *CVPR*, 2019. 2, 6, 7

[39] Paul Voigtlaender, Michael Krause, Aljosa Osep, Jonathon Luiten, Berin Balachandar Gnana Sekar, Andreas Geiger, and Bastian Leibe. Mots: Multi-object tracking and segmentation. In *CVPR*, 2019. 3

[40] Paul Voigtlaender and Bastian Leibe. Online adaptation of convolutional neural networks for video object segmentation. In *BMVC*, 2017. 3

[41] Qiang Wang, Yi He, Xiaoyun Yang, Zhao Yang, and Philip Torr. An empirical study of detection-based video instance segmentation. In *ICCVW*, 2019. 2

[42] Wenguan Wang, Hongmei Song, Shuyang Zhao, Jianbing Shen, and Haibin Ling. Learning unsupervised video object segmentation through visual attention. In *CVPR*, 2019. 3

[43] Nicolai Wojke, Alex Bewley, and Dietrich Paulus. Simple online and realtime tracking with a deep association metric. In *ICIP*, 2017. 6, 8

[44] Jialian Wu, Liangchen Song, Tiancai Wang, Qian Zhang, and Junsong Yuan. Forest r-cnn: Large-vocabulary long-tailed object detection and instance segmentation. In *ACM Multimedia*, 2020. 3

[45] Saining Xie, Ross Girshick, Piotr Dollár, Zhuowen Tu, and Kaiming He. Aggregated residual transformations for deep neural networks. In *CVPR*, 2017. 8

[46] Yuwen Xiong, Renjie Liao, Hengshuang Zhao, Rui Hu, Min Bai, Ersin Yumer, and Raquel Urtasun. Upsnet: A unified panoptic segmentation network. In *CVPR*, 2019. 3

[47] Ning Xu, Linjie Yang, Yuchen Fan, Dingcheng Yue, Yuchen Liang, Jianchao Yang, and Thomas Huang. Youtube-vos: A large-scale video object segmentation benchmark. *arXiv*, 2018. 2

[48] Zhenbo Xu, Wei Zhang, Xiao Tan, Wei Yang, Huan Huang, Shilei Wen, Errui Ding, and Liusheng Huang. Segment as points for efficient online multi-object tracking and segmentation. In *ECCV*, 2020. 3

[49] Linjie Yang, Yuchen Fan, and Ning Xu. Video instance segmentation. In *ICCV*, 2019. 1, 2, 4, 5, 6, 7

[50] Linjie Yang, Yanran Wang, Xuehan Xiong, Jianchao Yang, and Aggelos K Katsaggelos. Efficient video object segmentation via network modulation. In *CVPR*, 2018. 6

[51] Xiaohang Zhan, Xingang Pan, Bo Dai, Ziwei Liu, Dahua Lin, and Chen Change Loy. Self-supervised scene de-occlusion. In *CVPR*, 2020. 8

[52] Xizhou Zhu, Yuwen Xiong, Jifeng Dai, Lu Yuan, and Yichen Wei. Deep feature flow for video recognition. In *CVPR*, 2017. 3